

STUDY OF GEOMETRICAL CHARACTERISTICS EFFECTS ON RADIATION PROPERTIES IN HIGH POROSITY FIBROUS POROUS MEDIA USING THE PORE-SCALE SIMULATION AND TWO-FLUX MODEL

by

Seyed M. HOSSEINALIPOUR* and Mohammadmehdi NAMAZI

School of Mechanical Engineering, Iran University of Science and Technology, Tehran, Iran

Original scientific paper
<https://doi.org/10.2298/TSCI180722009H>

In the present study, the radiation properties of a high porosity fibrous medium which is used in catalytic heaters were estimated. The calculation process was based on an inverse method using pore scale simulation and two-flux model. The results showed a good agreement with available experimental results. The effects of geometrical parameters including the solid volume fraction, fibers orientation, and diameter on the radiation properties were investigated. By increasing the solid share in the fibrous porous medium, the extinction coefficient increased, in which the absorption growth rate was higher than the scattering growth rate. The effect of the fibers angle on the scattering was greater than its effect on the absorption. For each porosity, an extinction coefficient could be defined in which, by increasing the fibers diameter, the extinction coefficient would not be reduced any more. The solid volume fraction, fibers diameter, and orientation were found to be the most effective geometric parameters on the radiation properties, respectively.

Key words: *fibrous porous media, radiation properties, pore-scale simulation, inverse method, two-flux model*

Introduction

The variety of thermophysical properties of porous materials has led to a wide range of industrial applications. Fibrous medium which is made up of flexible solid fibers, is one of the most applicable porous materials. They are very common in thermal insulations [1]. The fibrous media with high porosity and specific surface area are used in catalytic combustion heaters [2]. In these types of heating systems, gas fuel and oxidizer flow through the fibrous structure containing catalyst. The surface catalytic combustion occurs by supplying the activation energy. In these gas heaters, CO and NO_x pollutants are reduced and combustion occurs with higher efficiency compared to conventional systems [3]. The radiation heat transfer becomes more significant by increasing the temperature in the combustion applications [4]. Hence, having the radiation heat transfer properties is consequential in order to calculate the performance of these systems more precisely.

The radiation properties of the porous media are the combination of the solid and fluid parts which can be obtained by different methods [5-8]. Since direct measurement of these properties is difficult, inverse method is commonly used as an alternative approach in which data obtained from experiments are used as inputs for the solutions of the governing equations [9]. Zhao *et al.* [10] used an inverse conduction-radiation analysis to determine the transient thermal

* Corresponding author, e-mail: alipour@iust.ac.ir

response of a fibrous insulation up to 980 K. Reddy and Somasundharam [11] used gaussian process regression technique to estimate the thermal properties of orthotropic materials. Although it is possible to calculate the properties of a specific medium using experimental data by the inverse method, a slight change in the pores structure leads to significant errors. In addition, it is time-consuming and costly to repeat the experiments for each new structure, Daryabeigi [12]. On the other hand, substitution of the experiments by exact solutions for porous media is not of great interest because of the hardware constraints. Simplifications are necessary to overcome this limitation which ends up with eliminating the complexity of the physical medium and thus limits the application of the results to simple structures, Tong and Tien [13]. In this case, the numerical studies can be beneficial. The geometrical characteristics of a porous medium affect the fluid-flow as well as heat and mass transfer, Ibrahim [14]. Therefore, it is necessary to consider geometrical details of porous structure in the numerical simulations of the transport phenomena. Tahir *et al.* [15] used Monte-Carlo ray tracing algorithm to study the role of microstructural parameters in radiative transmittance through fibrous insulations. Qashou *et al.* [16] studied the solid volume fraction (SVF) and fibers diameter effects on transient radiative heat transfer response in a fibrous insulation by a simple 2-D CFD model. However, it is still not feasible to consider the pores structural details in the whole physical domain because of high computational costs. A suitable method to overcome this limitation is called *pore-scale simulation*. This method is based on the simulation of a small part as the representative of the whole domain, considering the structural details and calculating the equivalent properties on this scale. This method is almost well known in studying transport properties in rocks, Di-Palmaa [17] and Vilcaes [18]. Tahir *et al.* [15] used this approach along with Monte-Carlo method in a fibrous medium to study the microstructural effects on transmittance.

The novelty of the present study was to propose and validate a quick approach for estimating the radiative properties in porous geometries. The radiation properties are calculated by an inverse method using pore scale simulation and two-flux model. In the presented approach there is no need to repeat the experiments for new geometrical characteristics. In addition, to fill the research gaps in the literature, the effects of geometric parameters were comprehensively studied on absorption, scattering, albedo and extinction coefficients for a fibrous media used for catalytic combustion application as a case study. The results can help both manufacturers and researchers to introduce more efficient systems to the market. Furthermore, the proposed approach can be generalized as a fairly quick method for other types of porous media such as sphere-packed and foams, which is among future works of the current project's research team.

Geometry generation

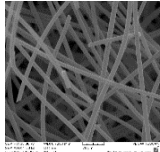
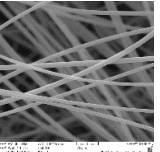
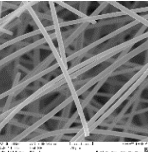
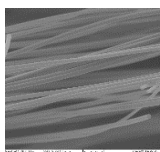
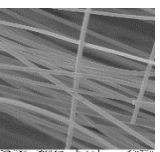
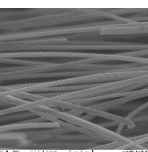
Three samples from a fibrous porous medium applicable for catalytic combustion made up of Al_2O_3 with more than $100 \text{ m}^2/\text{g}$ surface area were chosen and the pores structure and geometrical characteristics were determined using Tescan VEGA II – XMU SEM from different views, tab. 1. It was shown from vertical images that the fibers were distributed in all directions without any dominant distribution angle and a layered structure was observed from lateral view with no fibers penetration. Based on SEM measurements, more than 90% of the fibers had the diameter of 4-6 μm . A code was developed based on the algorithm proposed in [19] to generate the fibrous porous geometry. For simplicity purposes, here the diameter of 5 μm was considered for all of the fibers. The distribution of the fibers was not completely isotropic or layered but the later pattern was prevailing, tab. 1. Hence, the distribution angles were considered by a mean angle of 3° relative to the layered structure. The porosity of the medium was 0.987 based on manufacturer data sheet. To find the suitable size of simulation domain as a good representative of the main

medium, the Brinkman's length, $k^{1/2}$, was used. In which, k is the permeability of the medium and is calculated using Davies [20] and or Jackson and James [21] relations. A domain size about 14 times larger than the Brinkman's length is sufficient to smooth out local heterogeneities [22]. In the present study, the Brinkman's length was calculated as $230 \mu\text{m}$. So the minimum size of the computational domain has to be larger than $230 \mu\text{m}$, which is considered $300 \mu\text{m}$. To generate the fibers, following procedure was considered; a uniform probability function is used to choose a point randomly within the domain. Two angles θ and φ as orientation angles with z -axis and yz plane, respectively, are shown in fig. 1. The fiber axis can be plotted having a point and guessing two orientation angles. The new fiber axis could be drawn if the distances between the new axis with the other ones were not less than d_f (no penetration of the fibers). In each step, SVF could be calculated until the target SVF is reached. Figure 2 shows the fibers axis lines for $300 \mu\text{m}^3 \times 300 \mu\text{m}^3 \times 300 \mu\text{m}^3$ computational domain and SVF of 0.013.

Methodology

In order to investigate the effect of structural specifications on radiation properties, pore scale simulation is used along with the inverse method. First, equations including radiation effects are solved numerically by applying appropriate boundary conditions in the pore scale. After validating the simulation results, radiation intensity on boundaries can be calculated. Hence, the optical thickness of the medium can be determined using the Beer law [23]. Having the radiation intensities on boundaries and the isotropic scattering assumption inside the medium, the two-flux model can be solved in a loop by guessing the Albedo values ($0 < \omega < 1$) to calculate the radiation intensity at the opposite boundary. This process must be repeated until the difference between the radiation intensities calculated from the pore-scale simulation and

Table 1. The SEM images for different views (1000× zoom)

View	Sample #1	Sample #2	Sample #3
Vertical			
Lateral			

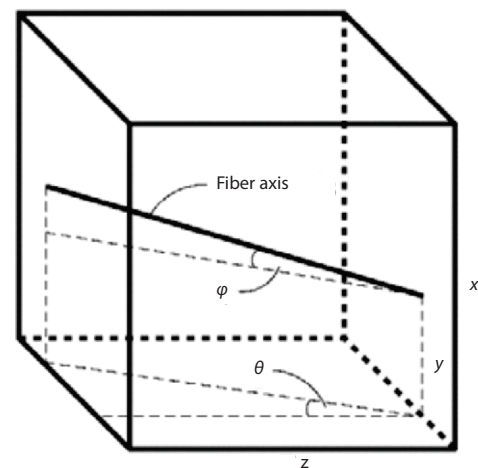


Figure 1. The fiber orientation angles in the computational domain

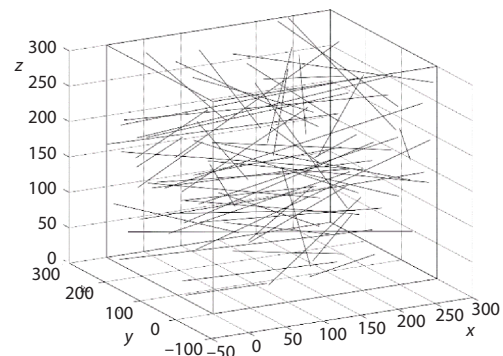


Figure 2. The fibers axis lines for $300 \mu\text{m}^3 \times 300 \mu\text{m}^3 \times 300 \mu\text{m}^3$ computational domain and SVF of 0.013

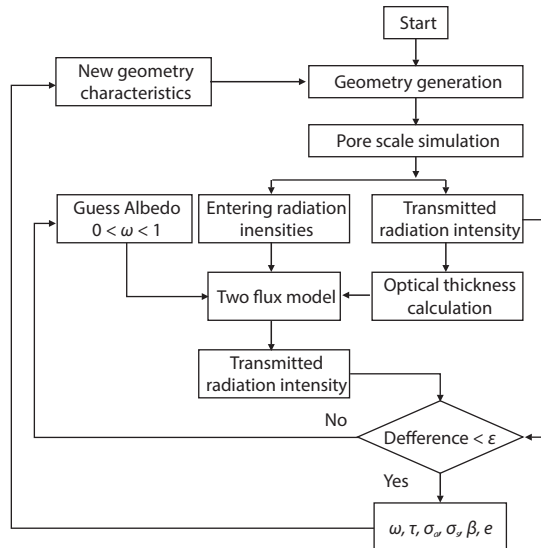


Figure 3. The methodology process for radiation properties estimation

two-flux model becomes negligible. Having the optical thickness and the Albedo coefficient, the absorption, scattering and extinction coefficients of the medium can be determined. Therefore, by changing the structural specifications of the medium, it is possible to study their effects on the radiation properties. The described algorithm is shown in fig. 3.

Assumptions, equations and boundary conditions

Pore scale simulation

In the present study no flow field is considered; *i. e.*, no pressure gradient and gravity field are applied. Hence, even natural-convection through simulation domain does not occur [24, 25]. Therefore, the problem can be modeled by the following eqs. (1) and (2):

$$0 = \frac{\partial}{\partial x_i} \left(k_g \frac{\partial T}{\partial x_i} \right) + S_g \quad (1)$$

$$0 = \frac{\partial}{\partial x_i} \left(k_s \frac{\partial T}{\partial x_i} \right) + S_s \quad (2)$$

Equations (1) and (2) are solved for fluid and solid, respectively. Nitrogen gas was considered to be confined among the fibers inside the simulation box. Since time variation behavior of the problem is not of interest, the steady form of the equations is employed. Temperature dependent thermal conductivity for nitrogen (as fluid) and alumina (as solid) were also considered. The S_g and S_s are source terms due to radiation heat transfer effects in fluid and solid, respectively. In the present study, gray medium assumption was applied in which properties

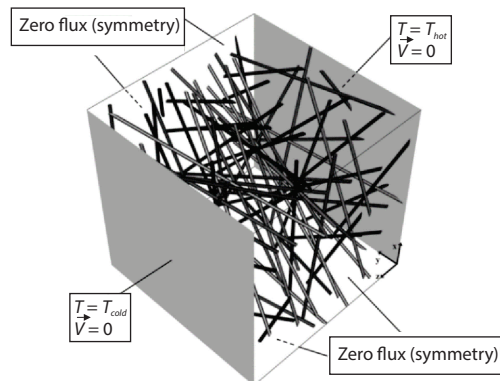


Figure 4. The computational domain and applied boundary conditions

are independent from wavelength. Considering the fibers surfaces as semi-transparent, radiation source terms are calculated using radiative transfer equation and discrete orientation model to include radiation effects. Hot and cold plates were considered at two opposite sides of the solution domain, same as the test conditions in the guarded hot plate method [25]. If the sample size is large enough, the choice of zero flux boundary condition does not affect the simulation results. This is because the heat fluxes are mainly in the through-plane direction and lateral heat fluxes are negligible [22, 26], fig. 4. The governing equations include only diffusion and source terms which were solved

numerically by control volume method using ANSYS FLUENT 13.0 [27]. The parallel computation option was used in a computer system with an Intel Core i7-4790 processor and 16 GB of RAM, which took about 30 minutes CPU time for each calculation. The residuals less than 10^{-6} as well as net heat flux at the boundaries were considered as two conditions for the convergence criteria and steady solution. To eliminate the effect of wall boundary condition (guarded hot plates) on the results, each pore scale simulation was repeated for computational domains with and without fibers which are shown schematically in fig. 5. In case, 5(a), the incident radiation intensity to the hot plate, emitted from the cold plate or $I_o^-(L) = I_o^-(\tau_L)$, and the incident radiation intensity to the cold plate, emitted from the hot plate or $I_o^+(0) = I_o^+(\tau_L = 0)$, are calculated. In case, fig. 5(b), the incident radiation intensity to cold plate, (transmitted from the fibrous domain or $I^+(L) = I^+(\tau_L)$, is determined. Using the emitted radiation intensity from the hot plate, $I_o^+(0)$, and the transmitted intensity from the fibrous domain, $I^+(L)$, in Beer's law, the fibrous domain optical thickness is computed.

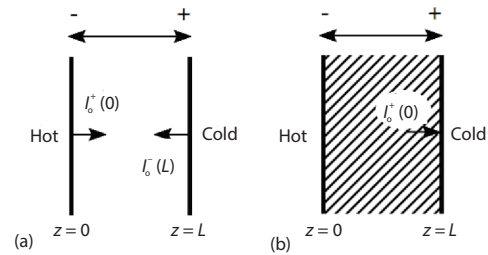


Figure 5. The pore scale simulations are repeated for two domains; (a) without considering the fibers, (b) with the fibers in the domain

Two-flux model and inverse method

The two-flux approximation is usually used for isotropically scattering media as in present study. Of course, one can also consider the case of the transport scattering function. This model is used here for Albedo calculations as eqs. (3) and (4):

$$\frac{dI^+}{d\tau} = -2(1-f\omega)I^+ + 2\omega bI^- + \frac{2n^2(1-\omega)\sigma T_b^4}{\pi} \quad (3)$$

$$\frac{dI^-}{d\tau} = +2(1-f\omega)I^- - 2\omega bI^+ - \frac{2n^2(1-\omega)\sigma T_b^4}{\pi} \quad (4)$$

Equations (3) and (4) form a set of first-order ODE which needs two boundary conditions to have a single solution which were obtained from pore scale simulation results. In two-flux model, the radiation intensity is considered in terms of optical thickness. However, we are seeking the radiative properties only for the optical thickness of the computational domain which is determined from pore scale simulations. Therefore, using two boundary conditions $I^-(\tau_L)$ and $I^+(0)$ (obtained from the pore scale simulations), by guessing a correct Albedo (ω), $I/303^+(\tau_L)$ can be calculated.

Radiation properties

Having the optical thickness, τ_L , and physical length of domain, L , extinction coefficient, β , can be calculated, $\tau_L = \beta L$. The calculated β and ω are used to compute σ_s , σ_a , $\omega = \sigma_s/\beta$, $\beta = \sigma_s + \sigma_a$.

Results

Model preparation

The fibers geometry was generated using a random technique. Therefore, it was necessary to check the repeatability of the generated geometry. For the characterization of the

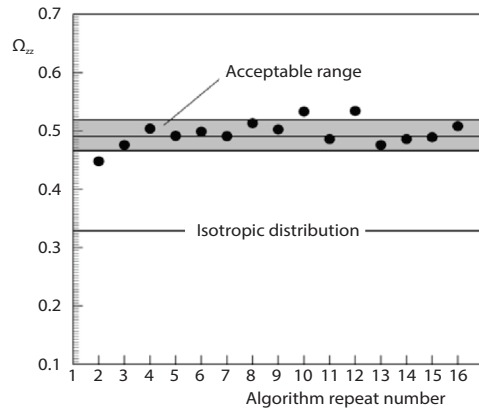


Figure 6. The Ω_{zz} results from 15 geometries generated with the same characteristics; the solid line is the results mean value; for the isotropic distribution $\Omega_{zz} = 0.33$

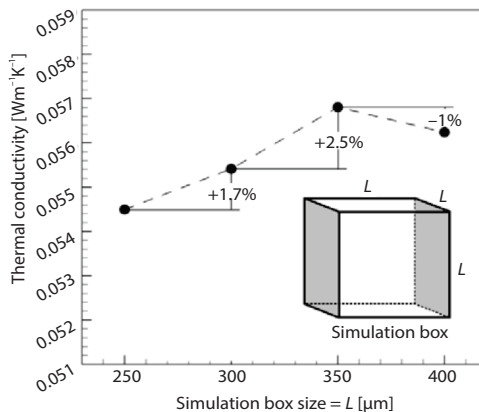


Figure 7. Effect of domain size of fibrous porous medium with SVF 1.3% on thermal conductivity coefficient

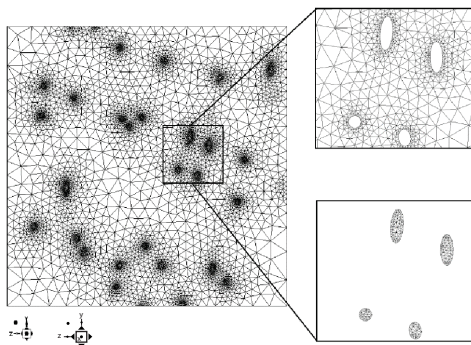


Figure 8. The mesh generated in a cross-section on yz-plane; the grids view is magnified separately for fluid and solid parts on the right two boxes

alignment degree of the fiber networks, the second-order fiber orientation tensor Ω , was employed [19]. The trace of Ω is always 1 and for the isotropic distribution, $\Omega_{xx} = \Omega_{yy} = \Omega_{zz} = 1/3$. In the present study, the fibers dominant alignment was in the z-direction. Hence, Ω_{zz} was used as a geometrical characteristic indicating a measure of fiber alignment in the z-direction. This was calculated for 15 geometries with the same characteristics by repeating the geometry generation algorithm. To evaluate the error, the simulations were repeated with the same boundary conditions on these 15 geometries. The thermal conductivity coefficient obtained from the geometries with $|\Omega_{zz} - \Omega_{zz,ave}| > 5\%$ differed more than 6.4% from the mean values of the simulations results. Hence, the use of a geometry in the simulation was acceptable only if the Ω_{zz} differed less than $\pm 5\%$ from the mean value, which is shown by grey field in fig. 6. Three geometries were not acceptable based on fig. 6. This process was repeated to ensure that the correct form of geometry was selected.

According to the characteristics of the fibrous medium in the present study and based on the Brinkman's length criterion, the minimum size of the computational domain was calculated to be 230 μm . To investigate the effect of computational domain size on effective thermal conductivity coefficient, fibrous medium was also generated in dimensions of 250 μm , 300 μm , 350 μm , and 400 μm with the same specifications, including porosity, fibers diameter and orientation. It should be noted that the mesh density around the fibers in all dimensions was five points on each fiber perimeter. The corresponding results are presented in fig. 7. Increasing the size of domain to larger than 300 μm led to 2.5% deviation for the thermal conductivity coefficient. Hence, 300 μm domain size was employed as the representative of the whole medium and was used for the simulations.

The generated fibrous domain had a complex geometry, fig. 2. Hence, ANSYS ICEM CFD 13.0 and tetrahedral mesh type were used for meshing the computational domain. Fixing 10 points on the perimeter of each fiber

cross-section start mesh generation led to 8463788 computational cells. Beyond this number, no considerable variation ($\approx 1\%$) was observed in the effective thermal conductivity coefficient as a criterion. A cross-section on yz -plane is shown in fig. 8 in which the grids view is magnified separately for fluid and solid parts to be distinguishable.

Model validation

In order to use experimental results presented by Daryabeigi [6, 12, 25], the medium density was considered to be 48 kg/m^3 and nitrogen gas with the pressure of 0.67 kPa was considered as the fluid occupying the porous medium. The thermal conductivity of the nitrogen gas increases with temperature, and in contrast, it has a decreasing trend in alumina. Since the solid fraction is very small ($SVF = 1.3\%$), the thermal conductivity of the nitrogen gas is dominant and the overall thermal conductivity will be more pronounced with temperature increase. On the other hand, according to Stefan Boltzmann's law of radiation, in higher temperatures, the thermal radiation is more influential, which leads to higher heat transfer rates in the medium. It should be noted that the equivalent thermal conductivity calculation was based on diffusion approximation which traditionally, is derived for a medium with a spatially constant refractive index [28]. On the other hand, the computational domain was included the nitrogen gas and distributed alumina solid fibers that made the refractive index change locally. By increasing the temperature, the radiation effect becomes more significant and this causes more difference between the simulation and the experimental results in the higher temperatures which reaches 22%. However, according to the application in this study, the temperature range is less than 1000 K and so the simulation results are only acceptable in the range of performance for catalytic combustion heaters, fig. 9. The results of the specific extinction coefficient show a good agreement with the experimental results by an average difference of 10% , fig. 10. Increasing the temperature not only increases the reflection from the fibers, but also increases the absorption. However, due to the low solid share and the very low impact of nitrogen gas in the radiation mechanism [29], the extinction coefficient increases with a slight slope.

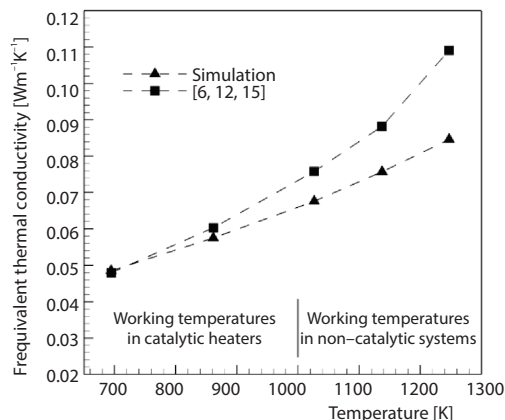


Figure 9. The simulation and experimental results of equivalent thermal conductivity as a function of temperature

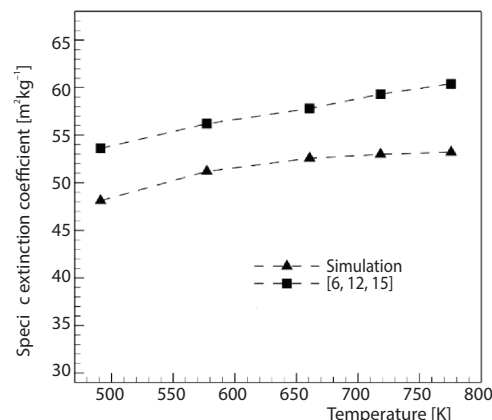


Figure 10. The simulation and experimental results of specific extinction coefficient as a function of temperature

Solid volume fraction

Four geometries with different SVF (1.3%, 4%, 7%, and 10.6%) were generated using the same algorithm and geometric specifications. In order to facilitate the meshing in the higher SVF geometries, the diameter of the fibers in all samples was fixed at 10 μm . Due to the fact that nitrogen gas has no significant effect on radiation mechanism, the absorption coefficient increases by increasing solid share. With the constant diameter of the fibers, by increasing the SVF, the number of fibers increases, which leads to an increase in the effective surface of the fibers for absorption, fig. 11. On the other hand, by increasing the number of fibers, the radiation scattering possibility in the fibrous medium becomes higher as the barriers for radiation have been increased. It should be noted that by increasing the solid share, scattering growth rate is decreased. The main reason is the increase in absorption observed in higher solid shares, which reduces the share of the scattering. With a very simple estimation of overall extinction coefficient in a porous medium, one can use the volume averaging of the extinction coefficients of each solid and fluid share in the medium. But our simulations and the literature [12, 25] do not confirm this linear relation. According to fig. 12, as well as the direct relation between absorption and scattering coefficients with SVF, fig. 11, the extinction coefficient increases non-linearly by increasing the SVF. The non-linear behavior observed in fig. 12 correctly shows that by increasing the solid share, the growth rate of radiation extinction decreases. In other words, by increasing the solid share, the extinction coefficient of the porous medium tends to the pure solid extinction coefficient. The Albedo coefficient is the ratio of the scattering coefficient to the sum of the absorption and scattering coefficients and decreases with respect to how these two coefficients increase. The important consequence is that, by increasing the solid share in the fibrous porous medium, the extinction coefficient increases, in which the absorption growth rate is higher than the scattering growth rate.

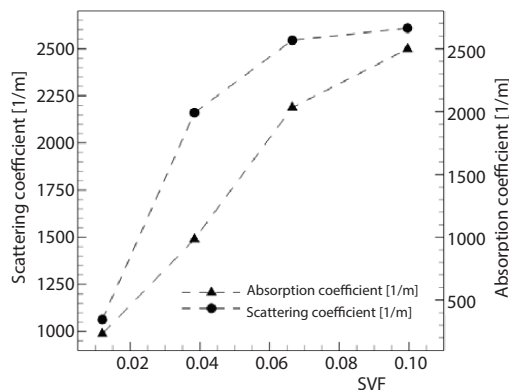


Figure 11. The absorption and scattering coefficients vs. SVF at 450 K

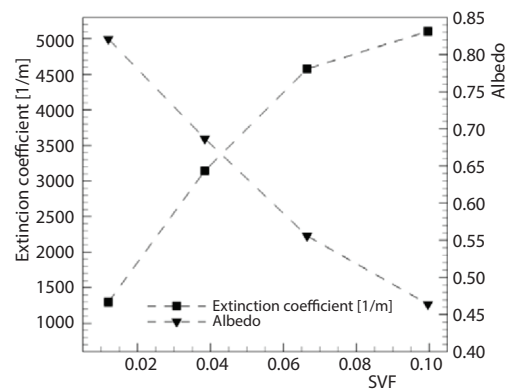


Figure 12. The extinction and Albedo coefficients vs. SVF at 450 K

Fibers orientation

From SEM results, tab. 1, it is determined that the fibers have an approximately uniform distribution in a plane perpendicular to the temperature gradient (xy -plane). Therefore, the distribution of fibers in the xy plane was considered the same. Hence, only the orientation of the fibers along the thermal flux (xy plane) was changed. The angles of 10°, 30°, 45°, 60°, and 90° with the boundary condition of 300 K and 800 K were chosen. Figure 13 shows

three fibers distribution from different direction views. According to fig. 14, with the increase in the angle of the fibers, the absorption and scattering coefficients decrease. Therefore, it could be expected that the extinction coefficient would be reduced. According to fig. 15 and also the Albedo coefficient definition, with the increase of the fibers angle, the reduction rate of the denominator (absorption + scattering) is greater than the numerator reduction (scattering). Therefore, the Albedo coefficient will slightly increase. In other words, the effect of the fibers angle on the scattering is greater than its effect on the absorption. Particularly from $\theta = 45^\circ$ to 90° , absorption was changed less than scattering. This made the scattering be the dominant parameter and as it influences denominator and numerator, albedo remained approximately constant.

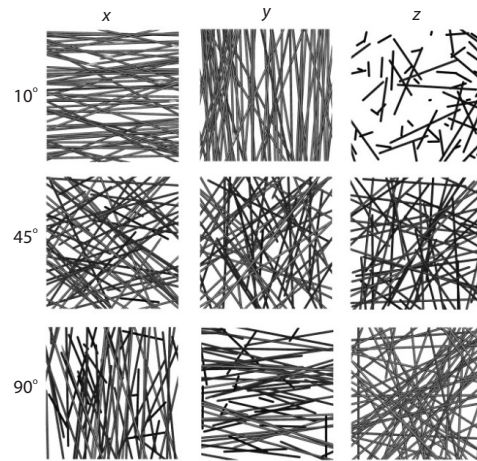


Figure 13. The fibers distribution for $\theta = 10^\circ$, 45° , and 90° from different direction views

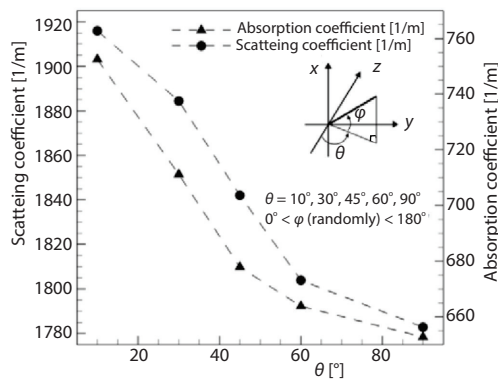


Figure 14. The absorption and scattering coefficients vs. z -direction orientation angle θ at 550 K

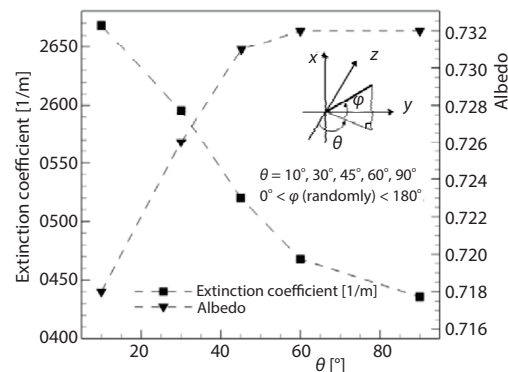


Figure 15. The extinction and Albedo coefficients vs. z -direction orientation angle θ at 550 K

Fibers diameter

The effect of fiber diameter on radiant properties was evaluated for the SVF of 1.3% and samples with fibers diameters of 5 μm , 7 μm , 8.5 μm , and 10 μm . Due to the fact that the volume of solid is constant, with increasing fibers diameter, the number of fibers reduces, which will reduce the effective surface for absorption/scattering of the radiation. Hence, the absorption and scattering coefficients show a decreasing trend, fig. 16. To describe the non-linearity of the variation, assume a cylinder with the length, L , and diameter, d , which is divided to m cylinders with the same length, L , and diameter, d' . But the same SVF leads to $d = (m)^{1/2}d'$. This relationship indicates that the side surface of the cylinder(s), which effectively influences the absorption and scattering, has a decreasing trend with increasing number of cylinders in constant solid volume, equivalent to decreasing diameter in constant SVF, ($p' = (m)^{1/2}p$, $m > 1 \Rightarrow p' > p$). But, as stated, this change is not linear. The radiation extinction coefficient, according to the relationship between absorption and scattering coefficients with fibers diameter, fig. 16,

decreases with increasing fibers diameter and shows a lower extinction in the fibrous porous medium with a larger diameter, fig. 17. The important point is that for each SVF, an extinction coefficient can be defined in which, by increasing the fibers diameter, the extinction coefficient will not be reduced any more. It can be seen in fig. 17 that the values of the Albedo have an incremental trend with respect to the increase in diameter.

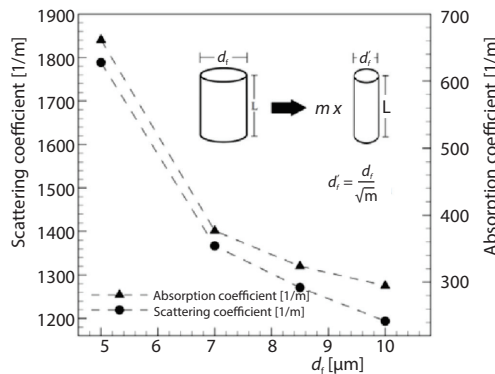


Figure 16. The absorption and scattering coefficients vs. fibers diameter at 550 K

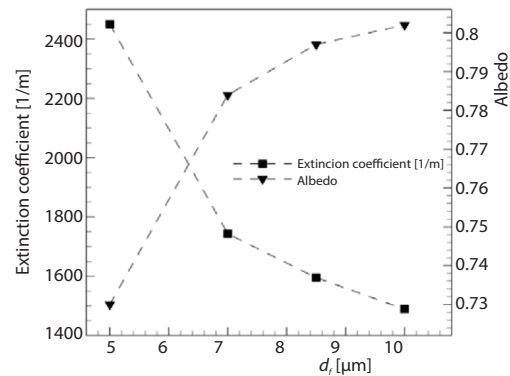


Figure 17. The extinction and Albedo coefficients vs. fibers diameter at 550 K

Table 2. The changes rate of the radiation properties based on changes in geometric characteristics

Parameter	Changes rate			
	σ_a	σ_s	β	ω
SVF	26729.4	16817.5	43546.8	-4.1
θ	-1.2	-1.8	-3.0	$1.7 \cdot 10^{-4}$
d_f	-72.2	-117.0	-189.2	$1.4 \cdot 10^{-2}$

does not have any physical meaning. But as a roughly approximation can be used to compare the geometrical characteristics effect. The SVF and θ have the most and the least effect on the radiant properties in the fibrous porous media, respectively. Therefore, in the optimal production process and in order to reduce the costs, it is suggested that the main focus should be on the SVF.

Conclusion

In this study, the radiation properties of a fibrous porous medium which is used in catalytic heaters were calculated by an inverse method using pore scale simulation and two-flux model. A geometry generation algorithm was proposed to model the fibrous porous medium at pore scale. By increasing the solid share in the fibrous porous medium, the extinction coefficient increases, in which the absorption growth rate is higher than the scattering growth rate. The effect of the fibers orientation on the scattering is greater than on the absorption. It seems that for each SVF, an extinction coefficient can be defined in which, the extinction coefficient will not be reduced any more by increasing the fibers diameter. The SVF, fibers diameter and orientation are, respectively the most effective geometric parameters on the radiation properties. The presented approach can be used as a fairly quick and simple tool to study the radiation

A very attractive point is to compare the effects from different parameters on the radiation properties. To do so, despite the fact that the changes were not linear, a linear curve was fitted on simulation results just for changes rate comparison. These rates are presented in tab. 2. It must be keep in mind that the reported rates

heat transfer properties in high porosity fibrous or other types of porous media. This can help to produce more effective porous material for specific applications.

Acknowledgment

This work was supported by Energy, Water and Environment Research Center Lab. in Iran University of Science and Technology.

Nomenclature

d_f	– fiber diameter, [m]
e	– specific extinction coefficient, [m^2kg^{-1}]
f	– forward scattering ratio, [–]
I^+, I^-	– forward and Backward radiation intensity, [WSr^{-1}]
k	– permeability, [m^2]
k_g	– thermal conductivity for gas, [$\text{Wm}^{-1}\text{K}^{-1}$]
k_s	– thermal conductivity for solid, [$\text{Wm}^{-1}\text{K}^{-1}$]
L	– characteristic length, [m]
n	– refractive index, [–]
T	– temperature, [K]

x_i, x_j – spatial components, [m]

Greek Symbols

β	– extinction coefficient, [m^{-1}]
θ	– horizontal angle, [$^\circ$]
σ	– Stefan-Boltzmann constant, [$\text{Wm}^{-2}\text{K}^{-4}$]
σ_a	– absorption coefficient, [m^{-1}]
σ_s	– scattering coefficient, [m^{-1}]
τ	– optical thickness, [–]
φ	– vertical angle, [$^\circ$]
ω	– Albedo, [–]
Ω	– fiber orientation tensor, [–]

References

- [1] Akolkar, A., et al., Tomography Based Analysis of Conduction Anisotropy in Fibrous Insulation, *International Journal of Heat and Mass Transfer*, 108 (2017), B, pp. 1740-1749
- [2] Jodeiri, N., et al., Modelling a Counter-Diffusive Reactor for Methane Combustion, *Computers and Chemical Engineering*, 39 (2012), Apr., pp. 47-56
- [3] Reichelt, E., et al., Fiber Based Structured Materials for Catalytic Applications, *Applied Catalysis A: General*, 476 (2014), Apr., pp. 78-90
- [4] Malico, I., Pereira, F., Numerical Study on the Influence of Radiative Properties in Porous Media Combustion, *Journal of Heat Transfer*, 123 (2001), 5, pp. 951-957
- [5] Zhao, J., et al., Radiative Properties and Heat Transfer Characteristics of Fiber-Loaded Silica Aerogel Composites for Thermal Insulation, *International Journal of Heat and Mass Transfer*, 55 (2012), 19-20, pp. 5196-5204
- [6] Daryabeigi, K., et al., Heat Transfer Modelling for Rigid High-Temperature Fibrous Insulation, *Journal of Thermophysics and Heat Transfer*, 27 (2013), 3, pp. 414-421
- [7] Yuen, W., Cunningham, G., Radiative Heat Transfer Analysis of Fibrous Insulation Materials Using the Zonal-GEF Method, *Journal of Thermophysics and Heat Transfer*, 21 (2007), 1, pp. 105-113
- [8] Arambakam, R., et al., Dual-Scale 3-D Approach for Modelling Radiative Heat Transfer in Fibrous Insulations, *International Journal of Heat and Mass Transfer*, 64 (2013), Sept., pp. 1109-1117
- [9] Ozisik, M. N., Orlande, H., *Inverse Heat Transfer-Fundamentals and Applications*, Taylor and Francis, Abingdon, UK, 2000
- [10] Zhao, S., et al., An Inverse Analysis to Determine Conductive and Radiative Properties of a Fibrous Medium, *Journal of Quantitative Spectroscopy and Radiative Transfer*, 110 (2009), 13, pp. 1111-1123
- [11] Reddy, K. S., Somasundharam S., An Inverse Method for Simultaneous Estimation of Thermal Properties of Orthotropic Materials Using Gaussian Process Regression, *Journal of Physics: Conference Series*, 745 (2016), 3, 032090
- [12] Daryabeigi, K., Thermal Analysis and Design Optimization of Multilayer Insulation for Reentry Aerodynamic Heating, *Journal of Spacecraft and Rockets*, 39 (2002), 4, pp. 509-514
- [13] Tong, T., Tien, C., Radiative Heat Transfer in Fibrous Insulations – Part I: Analytical Study, *Heat Transfer Journal*, 105 (1983), 1, pp. 70-75
- [14] Ibrahim, S. M., Radiation Effects on Mass Transfer Flow through a Highly Porous Medium with Heat Generation and Chemical Reaction, *ISRN Computational Mathematics*, 2013 (2013), ID765408
- [15] Tahir, M. A., et al., Modelling the Role of Microstructural Parameters in Radiative Heat Transfer through Disordered Fibrous Media, *International Journal of Heat and Mass Transfer*, 53 (2010), 21-22, pp. 4629-4637

- [16] Qashou, I., *et al.*, an Investigation of the Radiative Heat Transfer through Non-Woven Fibrous Materials, *Journal of Engineered Fibers and Fabrics*, 4 (2009), 1, pp. 9-15
- [17] Di-Palmaa, P., *et al.*, Pore-Scale Simulations of Concentration Tails in Heterogeneous Porous Media, *Journal of Contaminant Hydrology*, 205 (2017), Oct., pp. 47-56
- [18] Vilcaez, J., *et al.*, Pore-Scale Simulation of Transport Properties of Carbonate Rocks Using FIB-SEM 3-D Microstructure: Implications for Field Scale Solute Transport Simulations, *Journal of Natural Gas Science and Engineering*, 42 (2017), June, pp. 13-22
- [19] Stylianopoulos, T., *et al.*, Permeability Calculations in 3-D Isotropic and Oriented Fiber Networks, *Physics of Fluids*, 20 (2008), 12, p. 123601
- [20] Davies, C. N., The Separation of Airborne Dust and Particles, *Proceedings*, Institute of Mechanical Engineers B1, London, UK, 1952, pp. 185-213
- [21] Jackson, G. W., James, D. F., The Permeability of Fibrous Porous Media, *Canadian Journal of Chemical Engineering*, 64 (1986), 3, pp. 364-374
- [22] Wang, Q., *et al.*, Simulating through-Plane Permeability of Fibrous Materials with Different Fiber Lengths, *Modelling and Simulation in Materials Science and Engineering*, 15 (2007), 8, pp. 855-868
- [23] Mital, R., *et al.*, Measurements of Radiative Properties of Cellular Ceramics at High Temperatures, *Journal of Thermophysics and Heat Transfer*, 10 (1996), 1, pp. 33-38
- [24] Deutschmann, O., Computational Fluid Dynamics Simulation of Catalytic Reactors, in: *Hand Book of Heterogeneous Catalysis*, (Eds. Ertl, G., *et al.*), Wiley, USA, 2008, Chapter 6
- [25] Daryabeigi, K., *et al.*, Combined Heat Transfer in High-Porosity High Temperature Fibrous Insulations: Theory and Experimental Validation, *Journal of Thermophysics and Heat Transfer*, 25 (2011), 4, pp. 536-546
- [26] Jaganathan, S., *et al.*, A Realistic Approach for Modelling Permeability of Fibrous Media: 3-D Imaging Coupled with CFD Simulation, *Chemical Engineering Science*, 63 (2008), 1, pp. 244-252
- [27] Patankar, S., *Numerical Heat Transfer and Fluid-Flow*, CRC Press, Boca Raton, Fla., USA, 1980
- [28] Khan T., Jiang H., A New Diffusion Approximation the Radiative Transfer Equation for Scattering Media with Spatially Varying Refractive Indices, *Journal of Optics A: Pure and Applied Optics*, 5 (2003), Feb., pp. 137-141
- [29] Bockh, P., Wetzel, T., *Heat Transfer: Basics and Practice*, Springer-Verlag, Berlin, Heidelberg, Germany, 2012